


Generic two-phase coexistence in a type-2 Schloegl model for autocatalysis on a square lattice: Analysis via heterogeneous master equations

Zheren Shen ^{1,2}, Da-Jiang Liu ¹, and James W. Evans ^{1,2,3,*}

¹Ames National Laboratory - USDOE, Ames, Iowa 50011, USA

²Department of Mathematics, Iowa State University, Ames, Iowa 50011, USA

³Department of Physics & Astronomy, Iowa State University, Ames, Iowa 50011, USA

 (Received 2 November 2022; accepted 10 February 2023; published 3 March 2023)

Schloegl's second model (also known as the quadratic contact process) on a square lattice involves spontaneous annihilation of particles at lattice sites at rate p , and their autocatalytic creation at unoccupied sites with $n \geq 2$ occupied neighbors at rate k_n . Kinetic Monte Carlo (KMC) simulation reveals that these models exhibit a nonequilibrium discontinuous phase transition with generic two-phase coexistence: the p value for equistability of coexisting populated and vacuum states, $p_{\text{eq}}(S)$, depends on the orientation or slope, S , of a planar interface separating those phases. The vacuum state displaces the populated state for $p > p_{\text{eq}}(S)$, and the opposite applies for $p < p_{\text{eq}}(S)$ for $0 < S < \infty$. The special "combinatorial" rate choice $k_n = n(n-1)/12$ facilitates an appealing simplification of the exact master equations for the evolution of spatially heterogeneous states in the model, which aids analytic investigation of these equations via hierarchical truncation approximations. Truncation produces coupled sets of lattice differential equations which can describe orientation-dependent interface propagation and equistability. The pair approximation predicts that $p_{\text{eq}}(\max) = p_{\text{eq}}(S = 1) = 0.09645$ and $p_{\text{eq}}(\min) = p_{\text{eq}}(S \rightarrow \infty) = 0.08827$, values deviating less than 15% from KMC predictions. In the pair approximation, a perfect vertical interface is stationary for all $p < p_{\text{eq}}(S = \infty) = 0.08907$, a value exceeding $p_{\text{eq}}(S \rightarrow \infty)$. One can regard an interface for large $S \rightarrow \infty$ as a vertical interface decorated with isolated kinks. For $p < p_{\text{eq}}(S = \infty)$, the kink can move in either direction along this otherwise stationary interface depending upon p , but for $p = p_{\text{eq}}(\min)$ the kink is also stationary.

DOI: [10.1103/PhysRevE.107.034104](https://doi.org/10.1103/PhysRevE.107.034104)

I. INTRODUCTION

A comprehensive understanding of nonequilibrium discontinuous phase transitions in lattice models for stochastic interacting particle systems is still lacking [1–3]. Certain realizations of Schloegl's second model [4] on an infinite square lattice provide an excellent venue for fundamental analysis of such transitions [5–10]. In a general version of this model [10], one specifies a neighborhood, \mathcal{N} , for sites on the lattice consisting of N nearby sites. Then, particles residing at the sites of the lattice spontaneously annihilate at rate p , and particles are autocatalytically created at rate k_n at unoccupied sites only if those sites have $n \geq 2$ occupied sites or particles within their neighborhood \mathcal{N} [10]. Schloegl's original development of the models [4] was motivated by autocatalytic chemical reactions, wherein species are created and destroyed. The model also is equivalent to the quadratic contact process for spatial epidemics on a square grid of households [5]. In this model, households spontaneously recover from a disease at rate p , but can be infected by two or more sick neighbors. One common "threshold" rate choice sets $k_0 = k_1 = 0$, and $k_n = 1$ for all $n \geq 2$ [7–9]. Another combinatorial choice sets $k_n = \frac{\binom{n}{2}}{\binom{N}{2}} = \frac{n(n-1)}{N(N-1)}$, normalized so that the maximum rate is unity [10]. This combinatorial choice leads to an appealing exact reduction of the master equations, as discussed below,

and in this respect might be regarded as the most natural choice. This choice has also been described as the most natural generalization of the classic linear contact process [11]. Kinetic Monte Carlo (KMC) simulation of model behavior indicates that for either choice (and for some other choices), the model on an infinite lattice exhibits a discontinuous phase transition from a populated steady state to a vacuum absorbing state upon increasing p .

In addition, these and related models exhibit generic two-phase coexistence, i.e., there is not a unique value of $p = p_{\text{eq}}$ where the populated steady state and vacuum state are equistable and coexist [6,9,10]. This is in contrast to conventional equilibrium thermodynamic systems governed by Gibb's phase rule. Rather, p_{eq} , which corresponds to the p value where a planar interface separating coexisting populated and vacuum states is stationary, depends on the orientation or slope, S , of the interface. For planar interface orientations with $0 < S < \infty$, the interface begins to propagate when p deviates from p_{eq} , with the vacuum state displacing the populated state when $p > p_{\text{eq}}$, and the populated state displacing the vacuum state when $p < p_{\text{eq}}$.

Most studies of versions of Schloegl's second model on a square lattice have restricted attention to the case where \mathcal{N} just consists of the four nearest-neighbor sites, so that $N = 4$ [5–9]. It should be noted that any such model for $N = 4$ incorporates a "quirk" in that the populated steady state cannot displace the vacuum state separated from it by a planar vertical or horizontal interface (aligned with a principal

*Corresponding author: evans@ameslab.gov

lattice direction) no matter how small p [5,6,9,10]. Why? For square lattice sites labeled by (i, j) , suppose that sites with $i \geq 0$ correspond to the vacuum region separated by a vertical interface with slope $S = \infty$ from populated sites for $i < 0$. Sites with $i \geq 0$ can never become populated as they never have more than one populated neighbor. As a consequence, one finds that the vertical interface is stationary for all $p < p_{\text{eq}}(S = \infty)$, and the vacuum state displaces the populated state for $p > p_{\text{eq}}(S = \infty)$. For all other interface orientations defined by slope S , propagation in both directions can occur as p deviates from $p_{\text{eq}}(S)$.

Given the robustness of vacuum state against displacement by the populated state for vertical interfaces, one might anticipate that $p_{\text{eq}}(S = \infty)$ corresponds to the minimum $p_{\text{eq}}(\min) = \min_S p_{\text{eq}}(S)$, i.e., the vacuum state can survive for relatively low p . KMC studies show that this is the case for the *stochastic model* [6,9,10]. On the other hand, for diagonal interfaces with slope $S = 1$, one might anticipate that the vacuum state is most vulnerable to displacement by the populated state. For a perfect diagonal interface separating vacuum and fully populated state, each boundary site in the vacuum state has two potentially populated neighbors and thus is most susceptible to particle creation. As a result, one might expect that $p_{\text{eq}}(S = 1)$ corresponds to the maximum $p_{\text{eq}}(\max) = \max_S p_{\text{eq}}(S)$. KMC studies also show that this is the case [6,9,10].

In this paper, we restrict our attention to the combinatorial rate choice for particle creation on a square lattice where \mathcal{N} just consists of the four nearest-neighbor sites and $k_n = n(n-1)/12$. Thus, the nonzero particle creation rates are $k_2 = 1/6$, $k_3 = 1/2$, and $k_4 = 1$. Model behavior has been characterized previously by KMC simulation [10]. In particular, the KMC study demonstrated unambiguously that this particular stochastic model exhibits a discontinuous transition together with generic two-phase coexistence. Our goal here is to assess if an approximate analytic treatment is capable of capturing key features of the subtle model behavior, thereby providing deeper insight. Specifically, our analysis is based upon the hierarchical form of the exact master equations for the model. Given the need to assess the propagation of interfaces between populated steady state and the vacuum, these equations are unconventionally formulated to describe general spatially heterogeneous states. For spatially homogeneous states, hierarchical truncation using mean-field site approximation or the Kirkwood-type [12] pair approximation produces a closed set of rate equations describing kinetics. For spatially heterogeneous states, truncation produces a set of coupled lattice differential equations (LDEs) [13–16], although with unconventional spatial coupling [17–19], where these can describe interface propagation.

While LDEs have been used extensively to study interface propagation in spatially discrete models with nonlinear bistable kinetics, these invariably incorporate simple discrete Laplacian spatial coupling, and are based on simple mean-field models. In contrast, our generation of LDEs from truncation of exact master equations invariably produces more complex spatial coupling, even in the simplest mean-field approximation ignoring spatial correlations. Our higher-level treatment incorporating correlations using Kirkwood-type approximations produces coupled sets of LDEs which describe the evolution and variation across the interface of correlations as well as concentration. Determination of the regime of generic two-phase coexistence, $p_{\text{eq}}(\min) < p < p_{\text{eq}}(\max)$ from these LDEs is naturally of particular significance. One finds that $p_{\text{eq}}(\max) = p_{\text{eq}}(S = 1)$, which is determined straightforwardly from analysis of diagonal interfaces with $S = 1$. One the other hand, one finds that $p_{\text{eq}}(\min) = p_{\text{eq}}(S \rightarrow \infty) \neq p_{\text{eq}}(S = \infty)$, so determination of $p_{\text{eq}}(\min)$ requires a more delicate analysis of near-vertical interfaces as $S \rightarrow \infty$.

The exact master equations and the corresponding LDEs are presented in Sec. II as well as the site- and pair approximations. The site approximation captures qualitatively the basic features of the model, and the pair approximation captures these features semiquantitatively by accounting for spatial correlations. Our results from numerical integration analysis of the appropriate LDEs are presented in Sec. III. These in particular show that $p_{\text{eq}}(\min) < p_{\text{eq}}(S = \infty) < p_{\text{eq}}(\max)$. In Sec. IV, we provide additional insight into the model dynamics controlling $p_{\text{eq}}(\min) = p_{\text{eq}}(S \rightarrow \infty)$. An interface for large $S \rightarrow \infty$ can be regarded as a perfect vertical interface except for being decorated with isolated kinks. For $p < p_{\text{eq}}(S = \infty)$, the perfect vertical part of the interface is stationary, but the kink can move in either direction along this otherwise stationary interface depending upon p . However, the kink is shown to be stationary at a unique value of $p = p_{\text{eq}}(\min)$, as demonstrated by an LDE analysis of kink dynamics. Such an LDE-based kink-dynamics analysis is particularly instructive for elucidating subtle details of interface propagation in our model. Conclusions are provided in Sec. V.

II. HIERARCHICAL MASTER EQUATIONS AND THEIR TRUNCATION

A. General equations for spatially heterogeneous systems

Let $o[x]$ denote an unoccupied [occupied] site on the lattice, and $P(o_{i,j})$ [$P(x_{i,j})$] denote the probability that site (i, j) is unoccupied [occupied], $P(o_{i,j}o)$ denote the probability of a nearest-neighbor empty pair (i, j) , and $(i + 1, j)$, etc. Conservation of probability imposes relation including $P(o_{i,j}) + P(x_{i,j}) = 1$, $P(o_{i,j}o) + P(o_{i,j}x) = P(o_{i,j})$, etc. The “lowest-order” members of the exact hierarchical master equations have the form

$$\begin{aligned} d/dt P(o_{i,j}) = & + pP(x_{i,j}) - k_2 \left[P \begin{pmatrix} x & & \\ x & o_{i,j} & o \\ o & & \end{pmatrix} + P \begin{pmatrix} o & & \\ x & o_{i,j} & x \\ o & & \end{pmatrix} + P \begin{pmatrix} o & & \\ x & o_{i,j} & o \\ x & & \end{pmatrix} + \dots \right] \\ & - k_3 \left[P \begin{pmatrix} x & & \\ x & o_{i,j} & x \\ o & & \end{pmatrix} + P \begin{pmatrix} x & & \\ o & o_{i,j} & x \\ x & & \end{pmatrix} + P \begin{pmatrix} o & & \\ x & o_{i,j} & x \\ x & & \end{pmatrix} + P \begin{pmatrix} x & & \\ x & o_{i,j} & o \\ x & & \end{pmatrix} \right] - k_4 P \begin{pmatrix} x & & \\ x & o_{i,j} & x \\ x & & \end{pmatrix} \end{aligned}$$

$$= + pP(x_{i,j}) - k_2 \left[P \begin{pmatrix} \cdot & x \\ x & o_{i,j} \end{pmatrix} + P(x \ o_{i,j} \ x) + P \begin{pmatrix} x & o_{i,j} \\ \cdot & x \end{pmatrix} + P \begin{pmatrix} o_{i,j} & x \\ x & \cdot \end{pmatrix} + P \begin{pmatrix} x \\ o_{i,j} \\ x \end{pmatrix} + P \begin{pmatrix} x & \cdot \\ o_{i,j} & x \end{pmatrix} \right], \tag{1}$$

$$\begin{aligned} d/dt P(o_{i,j}o) &= + p[P(x_{i,j}o) + P(o_{i,j}x)] - k_2 \left[P \begin{pmatrix} x & x \\ x & o_{i,j} \\ o & o \end{pmatrix} + P \begin{pmatrix} o & o \\ x & o_{i,j} \\ o & o \end{pmatrix} + P \begin{pmatrix} x & o \\ o & o_{i,j} \\ o & o \end{pmatrix} \right] - k_3 P \begin{pmatrix} x & x \\ x & o_{i,j} \\ o & o \end{pmatrix} \\ &- k_2 \left[P \begin{pmatrix} o & x \\ o & o_{i+1,j} \\ o & x \end{pmatrix} + P \begin{pmatrix} o & o \\ o & o_{i+1,j} \\ x & x \end{pmatrix} + P \begin{pmatrix} o & x \\ o & o_{i+1,j} \\ o & o \end{pmatrix} \right] - k_3 P \begin{pmatrix} x & x \\ o & o_{i+1,j} \\ x & x \end{pmatrix} \\ &= + p[P(x_{i,j}o) + P(o_{i,j}x)] - k_2 \left[P \begin{pmatrix} x & o_{i,j} \\ \cdot & x \\ \cdot & \cdot \end{pmatrix} + P \begin{pmatrix} \cdot & x \\ x & o_{i+1,j} \\ \cdot & o \end{pmatrix} + P \begin{pmatrix} x & \cdot \\ o_{i,j} & o \\ x & \cdot \end{pmatrix} \right] \\ &- k_2 \left[P \begin{pmatrix} o & o_{i+1,j} \\ \cdot & x \\ \cdot & \cdot \end{pmatrix} + P \begin{pmatrix} \cdot & x \\ o & o_{i+1,j} \\ \cdot & x \end{pmatrix} + P \begin{pmatrix} \cdot & x \\ o & o_{i+1,j} \\ \cdot & x \end{pmatrix} \right]. \tag{2} \end{aligned}$$

$$d/dt P \begin{pmatrix} o_{i,j} \\ o \end{pmatrix} = + p \left[P \begin{pmatrix} x_{i,j} \\ o \end{pmatrix} + P \begin{pmatrix} o_{i,j} \\ x \end{pmatrix} \right] - \dots \tag{3}$$

All these equations for the probabilities of unoccupied configurations include gain (loss) terms from particle annihilation (autocatalytic creation). The simplified expressions for loss terms after the second equalities in (1) and (2) follow from exact reduction using conservation of probability. For example, in the simplified version of (1), the term

$$P \begin{pmatrix} \cdot & x \\ x & o_{i,j} \end{pmatrix} = P \begin{pmatrix} x & x \\ x & o_{i,j} \\ o & o \end{pmatrix} + P \begin{pmatrix} x & x \\ x & o_{i,j} \\ o & x \end{pmatrix} + P \begin{pmatrix} x & x \\ x & o_{i,j} \\ o & o \end{pmatrix} + P \begin{pmatrix} x & x \\ x & o_{i,j} \\ x & x \end{pmatrix} \tag{4}$$

is obtained by combining terms in the initial ‘‘primitive’’ expression, recalling that $k_2 = 1/6$, $k_3 = 1/2$, and $k_4 = 1$.

In the above hierarchy, the equation for the probability of a configuration of unoccupied sites couples to probabilities for configurations with a larger number of sites. To obtain equations involving a finite set of configuration sizes, truncation approximations can be implemented which account for possible spatial heterogeneity. In the simplest mean-field site approximation, the state of different sites is regarded as independent (i.e., all spatial correlations are ignored). Thus, one has that, e.g.,

$$P \begin{pmatrix} \cdot & x \\ x & o_{i,j} \end{pmatrix} \approx P(x_{i-1,j})P(o_{i,j})P(x_{i,j+1}) \cdot (\text{site}). \tag{5}$$

In the pair approximation, one accounts for nearest-neighbor site correlations, so that configuration probabilities are factorized as a product of the constituent pair probabilities compensating for double counting of shared sites between pairs. Thus, one has that, e.g.,

$$P \begin{pmatrix} \cdot & x \\ x & o_{i,j} \end{pmatrix} \approx P(x \ o_{i,j})P \begin{pmatrix} x \\ o_{i,j} \end{pmatrix} / P(o_{i,j}) \cdot (\text{pair}). \tag{6}$$

B. Truncation approximations for spatially homogeneous systems

For spatially homogeneous systems, further reduction of master equations is possible exploiting translational and rotational symmetry. For example, in (1), all four loss terms with bent trio configurations are equivalent, and the two loss

terms with linear trio configurations are equivalent. Applying the site approximation to (1) yields a closed equation for $P(o_{i,j}) = P(o)$ or equivalently for $P(x_{i,j}) = P(x) = C$, of the form $dC/dt = R(C) = -pC + (1-C)C^2$, where C denotes particle concentration. Steady-state analysis yields [10]

$$\begin{aligned} C_{\pm}(p) &= 1/2 \pm 1/2(1 - 4p)^{1/2} \quad \text{for} \\ p &\leq p_s(\text{site}) = 1/4, \quad \text{or} \quad C(p) = 0 \quad (\text{site}). \tag{7} \end{aligned}$$

C_+ is a stable populated state which coexists with a stable vacuum state, $C = 0$, for $p \leq p_s(\text{site}) = 1/4$ (the spinodal point, a saddle-node bifurcation). C_- is an unstable populated state. In the pair approximation, a natural variable is the conditional concentration, $K = P(x|o) = P(xo)/P(o)$, of an occupied site given an adjacent unoccupied site. Then, steady-state analysis yields

$$\begin{aligned} K_{\pm}(p) &= 1/2 \pm 1/2(1 - 8p)^{1/2} \quad \text{for} \\ p &\leq p_s(\text{pair}) = 1/8, \quad \text{or} \quad K(p) = 0 \quad (\text{pair}). \tag{8} \end{aligned}$$

One can obtain the corresponding $C(p)$ from the pair-approximation relation $C = 2K/(1 + K)$. Now, the stable populated state, K_+ , coexists with the stable vacuum state, $K = 0$, only up to the lower spinodal, $p_s(\text{pair}) = 1/8$. Note that these pair- (and site-) approximation results match those for the model on a Bethe lattice with coordination 4 [20].

KMC simulation of this stochastic Schloegl model on a square lattice reveals that p_{eq} varies from $p_{\text{eq}}(\text{min}) \approx 0.077$ to $p_{\text{eq}}(\text{max}) \approx 0.085$. The (strictly ill-defined) spinodal, p_s , should only be slightly above $p_{\text{eq}}(\text{max})$. This ‘‘weak

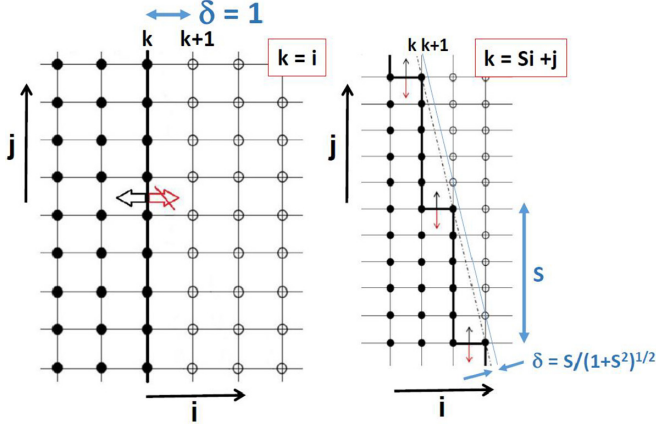


FIG. 1. Schematic: vertical interface (left) and an interface with slope $-S$ (right).

metastability,” associated with strong spatial correlations and fluctuations in the model, is in part due to the lack of diffusive mobility of particles [21]. The introduction of particle diffusion into the model would shift behavior towards mean-field behavior (7). New KMC studies indicate that $p_s \approx 0.096$ from an analysis of the kinetics of evolution to the vacuum state for $p = 0.098\text{--}0.120$, noting that the rate of “poisoning” is roughly proportional to $\Delta p = p - p_s$. See the Supplemental Material (SM) [22], Sec. SM1. Thus, $p_s(\text{pair}) = 0.125$ is much closer to the precise value $p_s \approx 0.096$ than $p_s(\text{site}) = 0.25$.

C. Truncation approximations for planar interfaces between steady states

For spatially heterogeneous systems, one must start with the general form of the hierarchical master equations. However, we will primarily consider the case of planar interfaces where there is some additional simplification. For example, for vertical interfaces one has that $P(x_{i,j}) = C_i$ depends only on i (and is independent of j), and below we replace i by k for uniformity. For an interface of slope $-S$ with $S = 1, 2, \dots$, one has that $P(x_{i,j}) = C_k$ depends only on $k = Si + j$. See Fig. 1. In the mean-field site approximation, where $d/dt C = R(C) = -pC + (1-C)C^2$ for homogeneous system, one has for vertical interfaces that

$$\begin{aligned} d/dt C_k &= -pC_k + 1/6(1 - C_k)[2C_k(C_{k+1} + C_{k-1}) \\ &\quad + C_{k-1}C_{k+1} + C_k^2] \\ &= R(C_k) + \square_\infty C_k \end{aligned} \quad (9)$$

For an interface of slope $-S$, one has that

$$\begin{aligned} d/dt C_k &= -pC_k + 1/6(1 - C_k)[(C_{k+1} + C_{k-1})(C_{k+S} + C_{k-S}) \\ &\quad + C_{k-1}C_{k+1} + C_{k-S}C_{k+S}] \\ &= R(C_k) + \square_S C_k \end{aligned} \quad (10)$$

Here, the spatial coupling term in (9) is $\square_\infty C_k = \frac{1}{3}(1 - C_k)C_k \Delta C_k + \frac{1}{6}(1 - C_k)(C_{k-1}C_{k+1} - C_k^2)$, where $\Delta C_k = C_{k+1} - 2C_k + C_{k-1}$ is the second-order difference.

The coupling term $\square_S C_k$ in (10) is also readily determined. Both $\square_\infty C_k$ and $\square_S C_k$ vanish for spatially homogeneous systems. Equations (9) and (10) have the form of lattice differential equations (LDEs), for which there is a vast literature analysis of associated interface propagation, although such studies almost exclusively choose spatial coupling terms of the simple form $\square C_k = D\Delta C_k$ [13–16].

In the pair approximation, one obtains from (1–3) coupled set of three lattice differential equations for C_i , $P(o_i o)$, and $P(o_i^o)$ for vertical interfaces [or C_k , $P(o_k o)$, and $P(o_k^o)$ for slope $-S$]. See Sec. SM2 [22] for details. These lattice differential equations will be applied to analysis of interface propagation when $p < p_s$ in the site- and pair approximations, as discussed in Sec. III.

III. LDE ANALYSIS FOR PLANAR INTERFACE PROPAGATION

For analysis of planar interface propagation when $p < p_s$ based on the LDEs, one can choose initial conditions with the homogeneous populated steady state on the “left” (for $k < 0$, say), and the vacuum state on the “right.” Note that as $P(o o) + P(x o) = P(o)$ and $P(x o) = K P(o)$, one can use $P(o o) = (1-K)(1-C)$ to generate the initial steady-state values of $P(o o)$ for the pair-approximation analysis. Then, from numerical integration of the LDE for $-L < k < +L$, with large L and suitable boundary conditions (e.g., fixing the variable at appropriate steady-state values), one can monitor interface propagation (for a range of times when the interface remains far from the boundaries $k = \pm L$). A convenient way to assess the propagation velocity normal to the interface, V_M , in such numerical analysis is to identify $V_M = \delta dM/dt$, where $M = \sum_k C_k / [C_+(p)]$ reflects the total amount of populated sites. Here, δ is the distance the interface travels (in the direction orthogonal to the interface) corresponding to the $\{C_k\}$ being replaced by $\{C_{k+1}\}$ or $\{C_{k-1}\}$. Thus, one has $\delta = 1$ for vertical interfaces, and $\delta = S/(1 + S^2)^{1/2}$ for interface slope S . See Fig. 1. We define the velocity to be positive when the populated state displaces the vacuum state, and negative when the opposite applies.

Using the case of a vertical interface for illustration, when $p < p_s$ is sufficiently high that the vacuum state displaces the populated state, one finds that after a transient period (reflecting the “sharp” interface initial conditions), V_M oscillates periodically in time. See Fig. 2 for pair-approximation results, and Sec. SM3 [22] for the corresponding site-approximation results. We extract a mean velocity, V , by averaging V_M over a period, τ , of oscillation. Equivalently, one can simply obtain V from the relation $V = 1/\tau$. See Sec. SM4 [22]. As noted above, the populated state cannot displace the vacuum state for vertical interfaces, so that $V \leq 0$ for all p . One finds that the interface is stationary for $p \leq p_{\text{eq}}(S = \infty) = 0.18469$ (site) or 0.08907 (pair), but the vacuum state displaces the populated state with $V < 0$ for $p > p_{\text{eq}}(S = \infty)$. Figure 2(c) shows pair-approximation predictions for this behavior of V versus p for a vertical interface.

It is appropriate to note that the oscillations in the interface velocity as determined by V_M could in some sense be regarded as an artifact of using changes in M to determine this

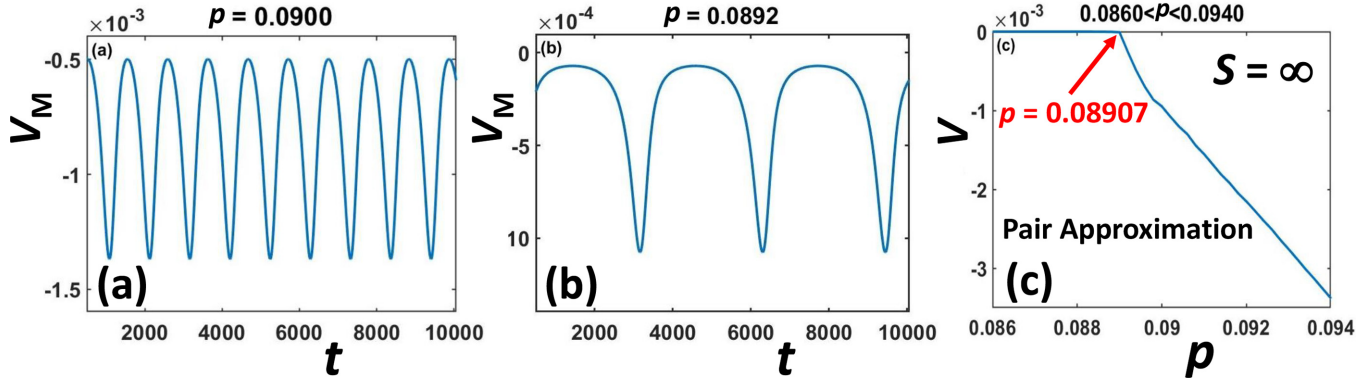


FIG. 2. Pair-approximation analysis of the propagation of a vertical interface ($S = \infty$). Periodic variation of V_M with t for: (a) $p = 0.0900$; (b) $p = 0.0892$ [which exceed $p_{eq}(S = \infty) = 0.08907$ so that the vacuum state displaces the populated state]. (c) Mean velocity, V , vs p .

velocity. The expectation for LDE, at least with the simple traditional choice of spatial coupling, is that propagating interface solutions have the form $C_k = F(\delta k - Vt)$. This has been demonstrated rigorously for spatial coupling $\square C_k = D\Delta C_k$ [23,24]. To assess whether this relation applies for our system, and if so to determine the form of F , we simply plot $C_k(t), C_{k+1}(t), C_{k+2}(t), \dots$ versus t for several adjacent sites. If the above relation applies, then these traces should have the same shape and just be shifted by an amount $\Delta t = \delta/V$ as k increases by 1. Figure 3 shows that this is the case in the pair approximation, and corresponding results for the site approximation are reported in Sec. SM3 [22]. Interestingly, as p approaches the point of propagation failure, $p_{eq}(S = \infty)$, F undergoes a transition from a smooth tanh-type form to a more complex structure. The latter is consistent with the feature that a “movie” of the propagating front just above $p = p_{eq}(S = \infty)$ suggests a stick-and-slip or stop-and-go type behavior. As an aside, we note that it is straightforward to show that any C_k with the general form $C_k = F(\delta k - Vt)$ produces an oscillating V_M (where V is the average V_M). See Sec. SM5 [22], illustrating this feature for a tanh form for F .

In Fig. 4, we provide comprehensive results for the variation of V with p for a range of different interface slopes $1 \leq S \leq \infty$. Note that for S increasing above $S = 1$, $p_{eq}(S)$ decreases monotonically from a maximum of $p_{eq}(S = 1) = 0.18782$

(0.09645) in the site (pair) approximation. The $p_{eq}(S)$ converge to a nonzero value, $p_{eq}(S \rightarrow \infty)$, which is strictly less than $p_{eq}(S = \infty)$. One has that $p_{eq}(S \rightarrow \infty) = 0.18077$ versus $p_{eq}(S = \infty) = 0.18469$ in the site approximation, and $p_{eq}(S \rightarrow \infty) = 0.08827$ versus $p_{eq}(S = \infty) = 0.08907$ in the pair approximation. In Table I, a comparison is presented of site- and pair-approximation predictions, and precise KMC results for p_{eq} versus slope, S . The pair approximation is quite effective in semiquantitatively recovering KMC results.

In Sec. I, we argued why the maximum p_{eq} should correspond to $S = 1$. This feature is captured by the LDE analysis (matching precise KMC results). However, appropriate interpretation of LDE results relative to KMC results for the minimum p_{eq} is more subtle. We argue that the precise $p_{eq}(\min)$ from KMC simulation corresponds to $p_{eq}(\min) = p_{eq}(S \rightarrow \infty)$ from the LDE analysis rather than the higher value $p_{eq}(S = \infty)$. The latter is “artificially elevated” by the feature that the analytic theory considered perfectly straight vertical interfaces where $C_{i,j}$ is independent of j . Fluctuations in the stochastic model imply that on-average vertical interfaces actually have some kink sites. This situation for vertical interfaces in the actual stochastic model is better captured by interfaces in the LDE treatment for finite but large S . In Sec. IV, we provide a more detailed analysis and physical interpretation of $p_{eq}(S \rightarrow \infty)$.

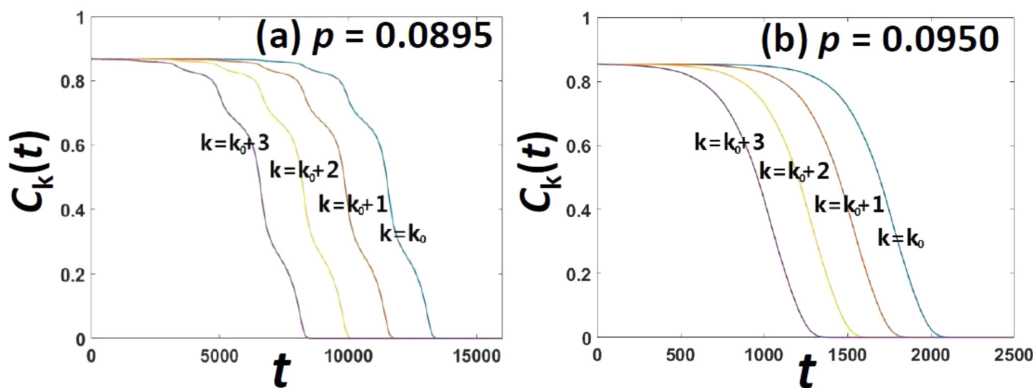


FIG. 3. $C_k(t)$ vs t for four consecutive $k = k_0, k_0 + 1, k_0 + 1, k_0 + 3$ for a propagation vertical interface in the pair approximation: (a) $p = 0.0895$; (b) $p = 0.0950$.

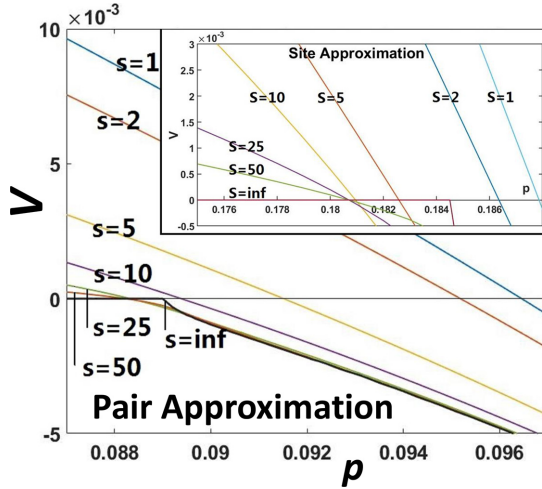


FIG. 4. V vs p for various S . Main figure: pair approximation. Inset: site approximation.

Finally, we note that “propagation failure” is a general phenomenon observed in LDE-based analysis of the evolution of interfaces which separate steady states in bistable systems [13–16]. This can occur over a finite range of control parameter (corresponding to p) for which the driving force for propagation is in some sense weak (even when no model quirk trivially blocks evolution as in our model for vertical interfaces). One might regard the feature that a vertical interface fails to propagate for all of $p < p_{\text{eq}}(S = \infty)$, rather than for just for $p < p_{\text{eq}}(S \rightarrow \infty)$, as a type of propagation failure. This view is supported by the following observation. One could perturb the model considered here in various ways to remove the “quirk” and allow the populated state to displace the vacuum state separated from it by a vertical interface. One possibility is to simply incorporate particle diffusion (hopping to unoccupied neighboring sites) or spontaneous particle creation at very small rate. Then, one still finds propagation failure of a vertical interface for a finite range of p centered around $p_{\text{eq}}(S \rightarrow \infty)$ (cf. Ref. [19]). This behavior will be described in more detail in a separate publication focused on more general models for $N = 4, 8, \dots$ and including spontaneous particle creation. In addition, analysis of LDEs for similar models indicates that interface propagation is also possible for $S = 1$, but only for an extremely narrow “negligible” range of width $\Delta p \sim 10^{-6}$ [19].

TABLE I. p_{eq} vs slope, S , for the site- and pair approximations vs precise KMC results.

	p_{eq} site	p_{eq} pair	p_{eq} KMC
$S = 1$	0.187 82	0.096 45	0.08494
$S = 2$	0.186 34	0.095 18	0.08413
$S = 3$	0.184 64	0.093 61	0.08274
$S = 4$	0.183 42	0.092 40	0.08198
$S = 5$	0.182 58	0.091 51	0.08115
$S \rightarrow \infty$	0.180 77	0.088 27	0.077
Spinodal	$p_s = 0.250$	$p_s = 0.125$	$p_s \approx 0.096$

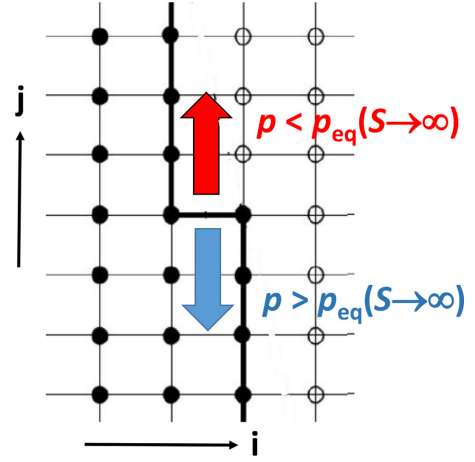


FIG. 5. Motion of an isolated kink on an otherwise vertical interface. $C_{i,j} = 0$ (o); $C_{i,j} > 0$ (\bullet). The schematic is idealized in that the actual $C_{i,j}$ does not suddenly become identically zero above the kink in the incomplete row along the step. See Fig. 8 for a realistic characterization.

IV. LDE ANALYSIS FOR KINK PROPAGATION DETERMINING $p_{\text{eq}}(\text{min}) = p_{\text{eq}}(S \rightarrow \infty)$

To elucidate behavior for V versus p from the LDE analysis for large S , we note that interfaces in this large- S regime can be regarded as vertical interfaces decorated with rare kink sites with separation $1/S$. Here, we consider $p < p_{\text{eq}}(S = \infty)$ so that a vertical interface is stationary. For such $p > p_{\text{eq}}(S \rightarrow \infty)$, these kinks will move in a direction along the otherwise stationary interface which expands the vacuum state, and for such $p < p_{\text{eq}}(S \rightarrow \infty)$ their motion expands the populated steady state. See Fig. 5. The point $p = p_{\text{eq}}(S \rightarrow \infty)$ should correspond to the special situation where an isolated kink (i.e., a single kink on an otherwise vertical interface) is stationary.

Thus, it is instructive to consider evolution for a vertical interface decorated by a single (completely isolated) kink in the regime $p < p_{\text{eq}}(S = \infty)$. However, the setup for the corresponding 2D LDE analysis is nontrivial, particularly the assignment of boundary conditions in the necessarily finite-size simulation system containing the kink. This is illustrated schematically in Fig. 6. A preliminary analysis is performed for a perfect vertical interface when $p < p_{\text{eq}}(S = \infty)$. We determine the nonzero steady-state values of $C_{i,j} = C_i$ for some $i < i^*$ (the location of the vertical interface), with $C_i \rightarrow C_+(p)$ as $i \rightarrow -\infty$, and where $C_i = 0$ for $i \geq i^*$. These C_i values are reported in Table II for $p = p_{\text{eq}}(S \rightarrow \infty)$ for the pair approximation.

Then, in the 2D system with an isolated kink, it is clear that the concentration profile for a perfect vertical interface will apply far from the kink site, where the profile will be shifted by one lattice constant to the left far above the kink relative to that far below the kink, as shown in Fig. 6. Thus, this nontrivial 1D concentration profile is used to assign upper and lower boundary concentrations as also indicated in Fig. 6 (where in numerical analysis both boundaries are ~ 100 lattice constants from the kink). Since C_i quickly approaches $C_+(p)$

TABLE II. $C_{i,j} = C_i$ for a vertical interface when $p = p_{eq}(S \rightarrow \infty)$ in the pair approximation.

Column	i^*-8	i^*-7	i^*-6	i^*-5	i^*-4	i^*-3	i^*-2	i^*-1	i^*
C_i	0.8706	0.8706	0.8705	0.8697	0.8652	0.8420	0.7309	0.3578	0

to the left of the interface, we assign $C_{i,j} = C_+(p)$ on the left boundary, about 10 lattice constants from the interface. The boundary condition on the right boundary is trivially $C_{i,j} = 0$.

From numerical integration of the 2D LDE for various $p < p_{eq}(S = \infty)$, we extract the propagation velocity, V_{kink} , of the kink along the interface versus p . Results are shown in Fig. 7 for the pair approximation, and in Sec. SM6 [22] for the site approximation. The key observation is that the p value for stationarity of the kink, $p_{eq}(kink)$, matches exactly $p_{eq}(S \rightarrow \infty)$ determined from an analysis of planar interface propagation. This applies in either the site- or pair approximation. In Fig. 8, we show the pair-approximation prediction for the distribution of time-independent concentrations $C_{i,j}$, in the vicinity of the stationary kink corresponding to $p = p_{eq}(S \rightarrow \infty)$. The kink is not sharply defined through a sudden change in concentration along the interface contrasting the idealized schematics, Figs. 5 and 6. The “smeared kink” is located in the rightmost column of Fig. 8 with nonzero $C_{i,j}$ entries, where one could assign the kink location (red ellipse) as where the concentration is ~ 0.17 midway between the limiting concentration values of 0 as $j \rightarrow +\infty$, and 0.357 as $j \rightarrow -\infty$ in this column. A more comprehensive listing of $C_{i,j}$ behavior in the pair approximation is provided in Sec. SM7 [22] which demonstrates convergence of the $C_{i,j}$ in rows far from the kink to the values for a perfect vertical interface reported in Table II.

V. CONCLUSIONS

Our formulation of Schloegl’s second model, also known as the quadratic process, on a square lattice with a combinatorial choice of rates is arguably the most natural extension of the linear contact model [11]. The model exhibits a nonequilibrium discontinuous phase transition between a populated state and a vacuum state, including the subtle phenomenon of generic two-phase coexistence. This phenomenon does not occur in thermodynamic systems as a result of the Gibbs phase rule. The combinatorial rate choice induces a simplification of the exact master equations which facilitates (but is not essential for) analytic treatment of the model. In the current contribution, we show that the pair approximation to the master equations for heterogeneous states is successful in recovering semiquantitatively the subtle features of model behavior, as determined precisely by KMC simulation. Our focus is on analysis of the dependence of the equistability value of $p = p_{eq}(S)$ for stationarity of a planar interface separating populated and vacuum steady states as a function of the slope, S . Of particular interest is determination of the regime of generic two-phase coexistence, $p_{eq}(min) = \min_S p_{eq}(S) < p < p_{eq}(max) = \max_S p_{eq}(S)$. Determination of $p_{eq}(max) = p_{eq}(S = 1)$ follows readily from an analysis for diagonal interfaces with $S = 1$. Determination of $p_{eq}(min) = p_{eq}(S \rightarrow \infty)$, which corresponds to equistability of near-vertical interfaces, is more subtle. Here, we show that $p_{eq}(min)$ can be assessed from analysis of the dynamics and stationarity of an isolated kink on an otherwise vertical interface. Results from the pair-approximation analysis are within 15% of precise values from KMC analysis.

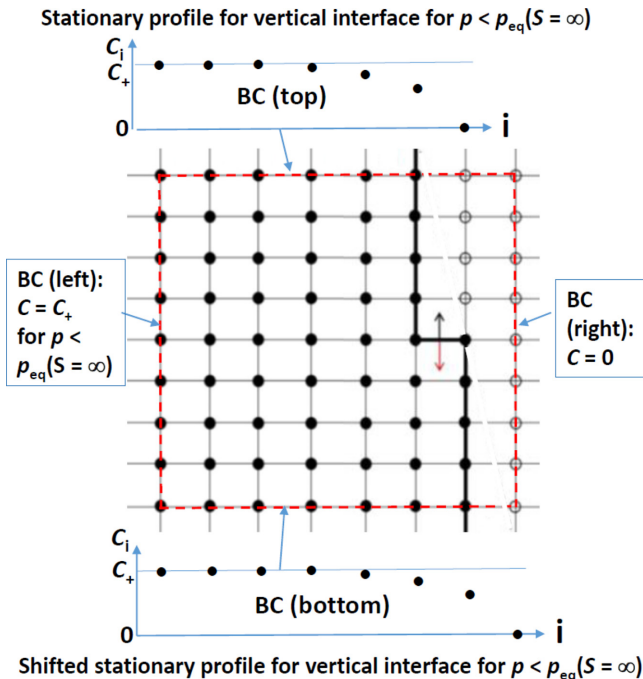


FIG. 6. Boundary conditions for 2D LDE analysis of the evolution of an isolated kink on a vertical interface.

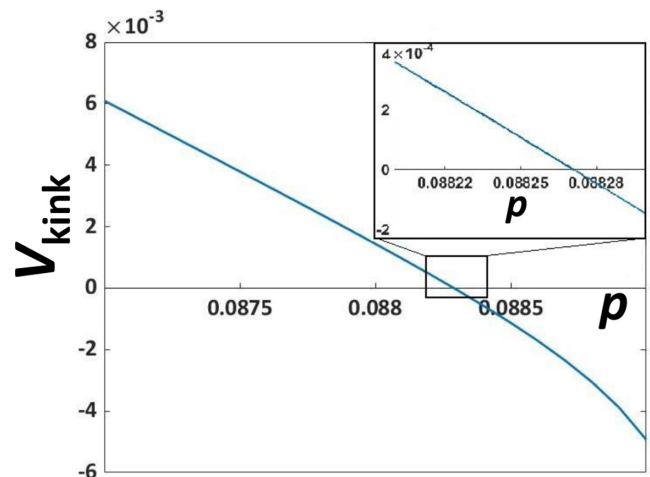


FIG. 7. Pair-approximation analysis of kink-propagation velocity, V_{kink} , along the vertical interface vs p . The kink is stationary when $p = 0.08827$ in the pair approximation.

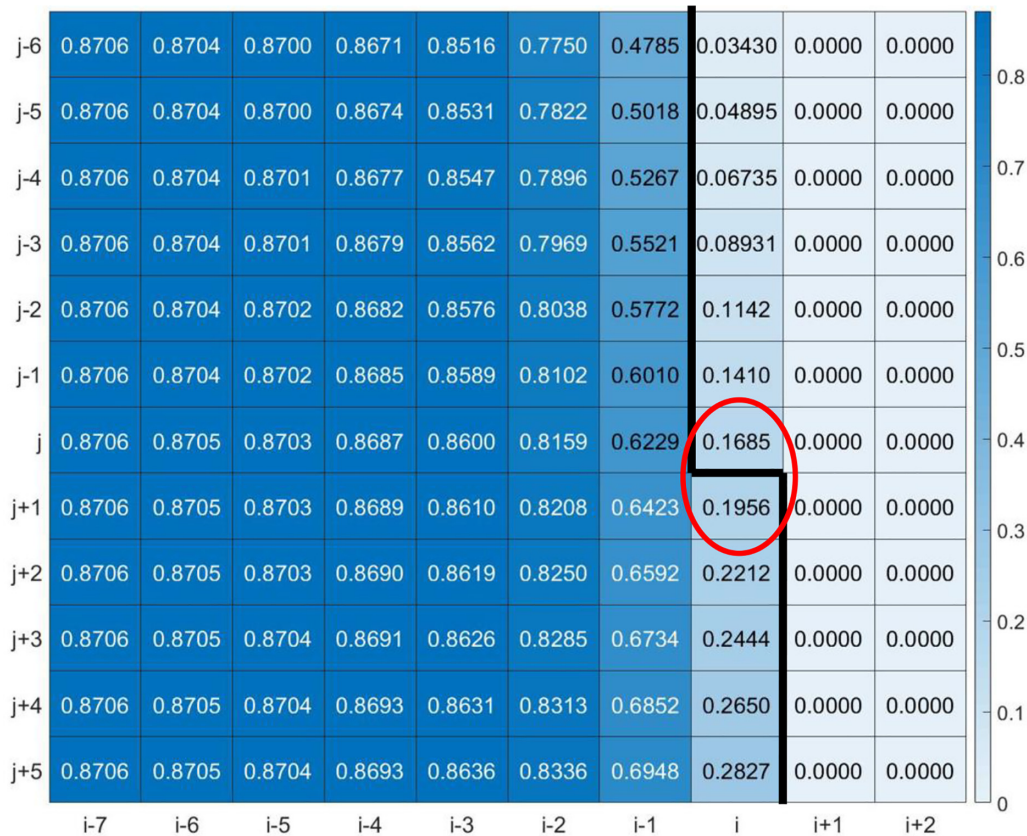


FIG. 8. Pair approximation prediction for $C_{i,j}$ in the vicinity of the stationary kink for $p = p_{\text{eq}}(S \rightarrow \infty)$. A color scale is also included to illustrate the variation in concentration, $C_{i,j}$.

ACKNOWLEDGMENTS

This research was supported by the USDOE, Office of Science, Basic Energy Sciences, Division of Chemical Sciences,

Geosciences, and Biosciences through the Computational & Theoretical Chemistry (CTC) project at Ames National Laboratory. Ames National Laboratory is operated by Iowa State University under Contract No. DE-AC02-07CH11358.

- [1] R. M. Ziff, E. Gulari, and Y. Barshad, *Phys. Rev. Lett.* **56**, 2553 (1986).
- [2] J. Marro and R. Dickman, *Nonequilibrium Phase Transitions in Lattice Models* (Cambridge University Press, Cambridge, 1999).
- [3] M. Henkel, H. Hinrichsen, and S. Luebeck, *Non-Equilibrium Phase Transitions* (Springer, Berlin, 2008), Vol. 1 Absorbing Phase Transitions.
- [4] F. Schloegl, *Z. Phys.* **253**, 147 (1972).
- [5] R. Durrett, *SIAM Rev.* **41**, 677 (1999).
- [6] D.-J. Liu, X. Guo, and J. W. Evans, *Phys. Rev. Lett.* **98**, 050601 (2007).
- [7] S. Handjani, *J. Theor. Probab.* **10**, 737 (1997).
- [8] E. F. da Silva and M. J. de Oliveira, *J. Phys. A: Math. Theor.* **44**, 135002 (2011), See Ref. [9] for contrasting results.
- [9] C.-J. Wang, D.-J. Liu, and J. W. Evans, *J. Chem. Phys.* **142**, 164105 (2015).
- [10] D.-J. Liu, C.-J. Wang, and J. W. Evans, *Phys. Rev. Lett.* **121**, 120603 (2018).
- [11] S. Chatterjee and R. Durrett, *Stoch. Processes Appl.* **123**, 561 (2013).
- [12] J. G. Kirkwood, *J. Chem. Phys.* **3**, 300 (1935).
- [13] S.-N. Chow, J. Mattel-Paret, and E. S. van Vleck, *Int. J. Bifurcation Chaos* **06**, 1605 (1996).
- [14] G. Fath, *Physica D (Amsterdam)* **116**, 176 (1998).
- [15] J. P. Keener, *SIAM J. Appl. Math.* **47**, 556 (1987).
- [16] J. W. Cahn, *Acta Met.* **8**, 554 (1960).
- [17] X. Guo, J. W. Evans, and D.-J. Liu, *Physica A (Amsterdam)* **387**, 177 (2008).
- [18] C.-J. Wang, D.-J. Liu, and J. W. Evans, *Phys. Rev. E* **85**, 041109 (2012).
- [19] C.-J. Wang, D.-J. Liu, and J. W. Evans, *Phys. Rev. E* **101**, 022803 (2020).
- [20] D.-J. Liu, C.-J. Wang, and J. W. Evans, *Phys. Rev. E* **104**, 014135 (2021).
- [21] J. W. Evans, D.-J. Liu, and M. Tammaro, *Chaos* **12**, 131 (2002).
- [22] See Supplemental Material at <http://link.aps.org/supplemental/10.1103/PhysRevE.107.034104> for description of KMC simulation assessing spinodal points in the stochastic models; LDE in the pair approximation; site-approximation analysis of interface propagation; interface propagation with constant velocity in discrete systems; analysis of kink propagation along an interface in the site- and pair approximations.
- [23] B. Zinner, *SIAM J. Math. Anal.* **22**, 1016 (1991).
- [24] B. Zinner, *J. Diff. Equations* **96**, 1 (1992).